

Incorporation of palladium nanoparticles and 10-molybdovanado phosphoric acid in FeCo layered double hydroxide structure: electrochemical and catalytic investigation for Mizoroki–Heck coupling reactions

Ezzat Rafiee^{1,2} · Masoud Kahrizi¹

Received: 17 April 2017 / Accepted: 16 June 2017 / Published online: 12 July 2017
© Springer Science+Business Media B.V. 2017

Abstract Palladium (Pd) has been immobilized on FeCo layered double hydroxide (LDH) intercalated 10-molybdovanado phosphate (FeCo/Mo₁₀V₂-Pd) for the first time. The structure was characterized using various characterization techniques. The electrocatalytic behavior of FeCo/Mo₁₀V₂-Pd was investigated using cyclic voltammetry and linear sweep voltammetry techniques. The presence of Mo₁₀V₂ enhanced the catalytic activity of FeCo-Pd in the Heck coupling reaction. Also, the collaboration of Pd and Mo₁₀V₂ with LDH as a mesoporous support was studied. These reusable solid catalysts exhibited excellent activity, and the methodology is applicable to diverse substrates providing good to excellent yields of the desired products. This method has advantages of high yields, low reaction times, elimination of ligand and base, heterogeneous catalysts and simple methodology. It is notable that FeCo/Mo₁₀V₂-Pd can easily separate from the reaction mixture using an external magnet and reused for at least four successive runs without any considerable decrease in its catalytic activity.

Keywords Layered double hydroxide · Mizoroki–Heck reaction · Heteropoly acid · Palladium · Cobalt-iron

Electronic supplementary material The online version of this article (doi:[10.1007/s11164-017-3013-5](https://doi.org/10.1007/s11164-017-3013-5)) contains supplementary material, which is available to authorized users.

✉ Ezzat Rafiee
e.rafeei@razi.ac.ir; Ezzat_rafeei@yahoo.com

¹ Faculty of Chemistry, Razi University, Kermanshah 67149, Iran

² Institute of Nano Science and Nano Technology, Razi University, Kermanshah 67149, Iran

Introduction

The Mizoroki–Heck coupling reaction plays an important role in carbon–carbon bond formation [1–3]. The palladium (Pd)-catalyzed Mizoroki–Heck reaction finds a lot of prominent positions in synthesis due to its exceptional versatility [4–6]. Nowadays, numerous kinds of Pd-based catalysts have been considered which have enabled this transformation to be applied with a broad substrate scope, a wide functional group tolerance and low catalyst loading. This reaction is generally considered to be a homogeneous reaction most commonly catalyzed by soluble Pd(II) species with a variety of ligands, such as palladium–phosphine complexes [7], oxime palladacycles [8], palladium–salen complexes [9], and palladium–N-heterocyclic carbene complexes [10]. Separation of the expensive catalyst from the product for reuse is often problematic in these homogeneous systems. Moreover, aggregation and precipitation of Pd metal in the homogeneous systems always leads to lost activity of the catalysts. Thus, heterogeneous catalysts are highly desirable, especially in large-scale synthesis, from both environmental and economic aspects. Much effort has been paid to developing heterogeneous catalytic systems that can be efficiently reused [11, 12]. Original ways have been found in the elaboration of magnetic catalysts that can be easily recovered using external magnets, and in the use of supported forms of catalytic systems without practical loss.

Immobilization of Pd nanoparticles on proper solid bases such as layered double hydroxides (LDHs) can help in the heterogenization of Pd species and provide many benefits in the catalytic properties of these catalysts [13–15].

LDH, namely hydrotalcite-like compounds, is a class of clay materials with positively charged metal-oxide layers, with the layer surface charges being balanced by interlayer anions [16–21]. The general formula for LDH is $[M_{(1-x)}^{2+}M_x^{3+}(-OH)_2][A^{m-}_{(x/m)}].nH_2O$, where M^{2+} and M^{3+} are divalent and trivalent metal cations and A^{m-} is a simple or complex anion such as Cl^- , NO_3^- , CO_3^{2-} or heteropoly acids (HPAs) [22–25]. The most attractive characteristic of LDHs is their anionic exchange ability where a wide range of organic or inorganic guests can be placed in the LDHs structures [26–28]. LDHs can provide “flexible” confining spaces that can be adjusted by changing the size and arrangement of the guest molecules. The flexible interlayer space can accommodate HPAs [29–31]. As the properties of the LDH can be altered based on the metal cations and interlayer anions, the applications of LDHs include catalysts, biomaterials, polymer additives, environmental materials (such as water treatment to ‘trap’ anionic pollutants), thin film applications, fire retardant additives, anticorrosion coatings, and controlled drug release in medications (with pharmaceutical compounds used as the interlayer anion) [32–39].

HPAs constitute a great family of inorganic oxo-metal clusters which are often composed of early transition metals [40–43]. The fascinating properties of HPAs make them attractive for application as catalysts [44]. Recently, HPAs have been widely used as nanomaterial catalyst in coupling reactions [45–48].

In continuation of our investigations into carbon–carbon coupling reactions [45–47], Pd immobilized on FeCo LDH intercalated 10-molybdovanado phosphate (FeCo/Mo₁₀V₂-Pd) was developed for the Mizoroki–Heck reaction.

Experimental

Material information

All reagents and solvents were commercially purchased from Fluka, Merck, and Aldrich. X-ray diffraction (XRD) patterns were recorded on an Inel French, EQUINOX 3000 model X-ray diffractometer using Cu-K radiation. Transmission electron microscopy (TEM) analysis was investigated using a TEM microscope (Philips CM 120 kV; Netherlands). Scanning electron microscopy (SEM) was studied using an AIS2300C microscope with a scanning range from 0 to 20 keV. Electron dispersive X-ray spectroscopy (EDX) measurements were made with an IXRF model 550i attached to the SEM. SEM samples were prepared by coating solid particles into a conductive layer. The magnetic properties of FeCo/Mo₁₀V₂-Pd were measured using a BHV-55 (Riken, Japan) vibrating sample magnetometer (VSM). Fourier transform infrared spectroscopy (FT-IR) spectra were recorded with KBr pellets using a Bruker ALPHA FT-IR spectrometer. The Pd and Mo content were evaluated using inductively coupled plasma atomic emission spectroscopy (ICP-AES) on a Spectro Ciros CCD spectrometer. The electrochemical behavior of the catalyst was measured using a computer-controlled m-Autolab modular electrochemical system (SAMA500 ElectroAnalyzer system). Thin layer chromatography (TLC) was carried out on pre-coated silica gel. Fluorescence of 254 nm (0.2 mm) on aluminum plates was used for monitoring the reactions. The cross-coupling products were characterized by their ¹H NMR spectra.

Preparation of FeCo LDH

FeCo LDH was prepared as follows: an aqueous alkaline solution (100 ml, 0.32 g Na₂CO₃, 0.48 g NaOH) was added to a mixed Fe³⁺ and Co²⁺ metal nitrate aqueous solution (Co²⁺/Fe³⁺ = 3.0 mol mol⁻¹) at 70 °C under vigorous stirring until the solution pH was adjusted to 10.0. The obtained slurry was then aged at 90 °C for 12 h. The resulting was cooled to room temperature and separated using external magnet, then frequently washed with distilled water and dried under vacuum.

Preparation of FeCo-Pd

FeCo-Pd was prepared by a deposition–precipitation procedure as follows: 0.5 g FeCo LDH was added to 255 ml PdCl₂ aqueous solution (0.008 M) and its pH was adjusted to 10.0 by the addition of 0.1 M NaOH and then positioned in a 80 °C water bath for 24 h. The resulting black slurry was recovered by a magnet, followed by washing with deionized water until no Cl⁻ remained, and then dried at 60 °C for 24 h to produce FeCo-Pd.

Preparation of FeCo/Mo₁₀V₂-Pd

Anion exchange reaction with the $[\text{PMo}_{10}\text{V}_2\text{O}_{40}]^{5-}$ (Mo_{10}V_2) anion was begun with the preparation of 50 ml of Mo_{10}V_2 (0.3 g) under N_2 atmosphere. Then, 1.00 g of FeCo-Pd was added to the previous solution. The mixture was kept under N_2 atmosphere and refluxed in the temperature range of 90–95 °C for 10 h. The resulting solid was separated by an external magnet and washed with boiling water three times, and then dried in vacuum.

General procedure for the Heck coupling reaction

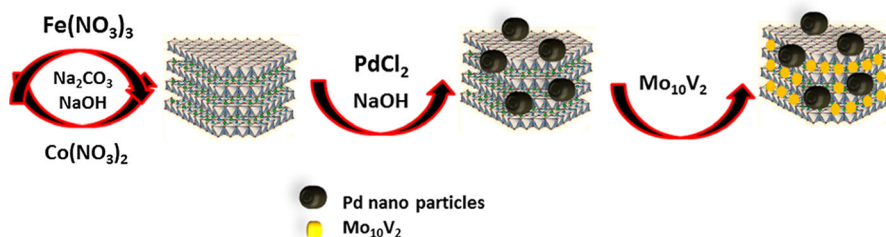
For the Heck coupling reaction, a mixture of aryl halide (4 mmol), styrene (4 mmol), tetrabutylammonium bromide, TBAB (4 mmol), FeCo/Mo₁₀V₂-Pd (0.02 g) and 5 mL dimethyl formamide (DMF) was charged to a reaction tube. The resulting mixture was refluxed at 120 °C under a dry N_2 atmosphere for an appropriate time. The progress of the reaction was monitored by TLC. Upon completion of the reaction, the mixture was then cooled to room temperature and FeCo/Mo₁₀V₂-Pd was separated by a magnet, washed with diethyl ether (2×10 mL), and then dried under vacuum for reuse. The residual mixture was extracted by CH_2Cl_2 (3×20 mL), and the combined organic layers were dried over MgSO_4 . The solvent was evaporated and the crude products were characterized by ^1H NMR spectroscopy [49].

Results and discussion

FeCo/Mo₁₀V₂-Pd was synthesized for the first time and used as a nanocatalyst for the Mizoroki–Heck reaction under base- and ligand-free conditions.

Scheme 1 shows the synthetic route for producing of the designed heterogeneous catalyst. The FeCo/Mo₁₀V₂-Pd was obtained by using a method that involves the separate synthesis of FeCo LDHs, immobilization of Pd nanoparticles on FeCo LDHs and intercalation of Mo₁₀V₂ in the FeCo-Pd structure.

In order to investigate the morphology of FeCo/Mo₁₀V₂-Pd, the catalyst samples have been studied by SEM (Fig. S1). It can be observed clearly from the SEM images that the fresh FeCo/Mo₁₀V₂-Pd presents well- developed, thin, flat crystals



Scheme 1 Synthetic route of FeCo/Mo₁₀V₂-Pd

with obvious edges indicating the layered structure (Fig. S1a, c). The SEM image of the catalyst shows the immobilization of Pd nanoparticles on layers of the catalyst. The mapping data of the catalyst provide a clear observation of the existence of the Pd nanoparticles, FeCo LDH and Mo_{10}V_2 in the structure of the char residue of FeCo/ Mo_{10}V_2 -Pd. Elementary analysis of the surface was studied by using EDX (Fig. S1i). This pattern of the catalyst shows major peaks of Co, Fe, Mo, V and Pd. The results obtained from the EDX analysis show the presence of FeCo LDH, Mo_{10}V_2 and Pd nanoparticles on the surface of the catalyst.

TEM images of FeCo/ Mo_{10}V_2 -Pd are shown in Fig. 1. Both images reveal the presence of small Pd nanoparticles deposited on the larger LDH flakes. The supported nanoparticles, covering the lower nanometer size range up to ca 25 nm, are highly dispersed.

Figure 2 shows the XRD patterns of FeCo LDH, Mo_{10}V_2 , FeCo/ Mo_{10}V_2 -Pd and the recovered FeCo/ Mo_{10}V_2 -Pd powders collected after fabrication. In the XRD pattern of FeCo LDH, strong diffraction peaks at 2θ of 11.06, 21.4°, 34.1°, 38.2°, 44.9°, 58.02° and 59.2° can be indexed to the (003), (006), (009), (012), (015), (110) and (113) facets of the LDHs, respectively, which are characteristic of a lamellar material (curve a) [50]. In order to show the presence of Mo_{10}V_2 in the catalyst, the XRD pattern of the Mo_{10}V_2 (curve b) is presented. After intercalation of Mo_{10}V_2 into the LDH layer, the diffraction pattern of the resulting material (curve c) shows a reflection characteristic of the LDH layer and Mo_{10}V_2 reflections. Curve c, after the Pd immobilization processes, shows the presence of Pd nanoparticles on the surface of the LDH. Pd(0) crystals in the catalyst have a crystalline structure with a peak appearing at 68.04° corresponding to the (220) plane of the Pd nanoparticles {JCPDS-05-0681}.

The presence of Mo_{10}V_2 in the LDH interlayers was identified by FT-IR. In natural LDHs before anion exchange processes, these interlayer anions are carbonate and water molecules [51]. In the FT-IR spectrum of FeCo LDH in addition to characteristic peaks of carbonate at about 1351 cm^{-1} , the absorption bands at 483 and 755 cm^{-1} which are attributed to the M–O vibration modes of the

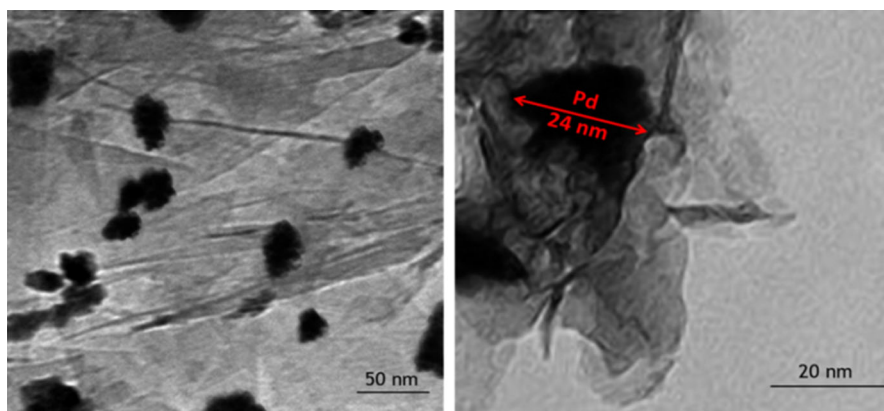


Fig. 1 TEM images of FeCo/ Mo_{10}V_2 -Pd

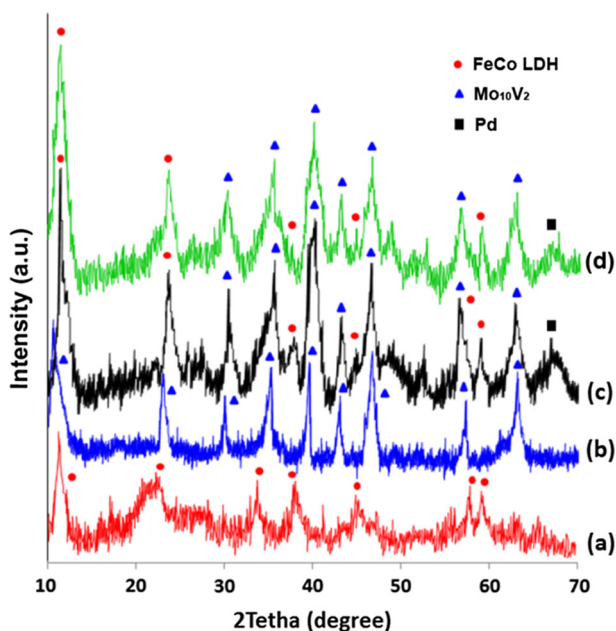


Fig. 2 XRD patterns of *a* FeCo LDH, *b* Mo₁₀V₂, *c* FeCo/Mo₁₀V₂-Pd, *d* recovered FeCo/Mo₁₀V₂-Pd

LDH structure were observed (Fig. S2a). Moreover, the band at 1630 cm^{-1} is attributed to the -OH stretching vibration related to the surface hydroxyl and H₂O. The FT-IR spectra of FeCo/Mo₁₀V₂-Pd, in addition to the FeCo LDH peaks at 492 and 768 cm^{-1} , display the features of a Keggin-type structure at 1057 , 1006 , 984 and 891 cm^{-1} which is in agreement with the results reported previously (curve Fig. S2b) [45]. Peaks at about 1351 cm^{-1} due to the carbonate band disappeared in the FeCo/Mo₁₀V₂-Pd sample, suggesting that the anion exchange was complete.

In order to evaluate the magnetic property of FeCo/Mo₁₀V₂-Pd, the VSM measurement was carried out at 298 K. Magnetization was saturated up to 30 emu/g at an applied field of 8500 Oe and reveals the superparamagnetic behaviors at room temperature (Fig. S3). The high magnetic property of FeCo/Mo₁₀V₂-Pd facilitates the recovery of the catalyst from the reaction media.

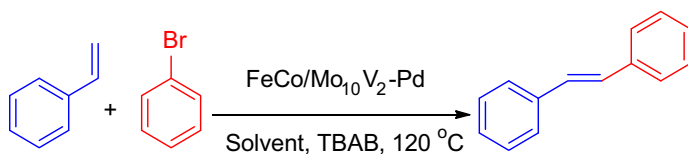
The electrocatalytic properties of FeCo LDH and FeCo/Mo₁₀V₂-Pd were studied in 0.1 M pH 4.0 phosphate buffers (PBS) by cyclic voltammetry (CV). Comparison of cyclic curves of FeCo LDH, FeCo-Pd and FeCo/Mo₁₀V₂-Pd (Fig. S4) shows the presence of Mo₁₀V₂. Enhancing the oxidation peak current of FeCo LDH decreased its oxidation peak potential from 0.41 and 0.34 in FeCo LDH and FeCo-Pd to 0.09 V in FeCo/Mo₁₀V₂-Pd, suggesting that the oxidation strength of FeCo LDH was facilitated by the presence of Mo₁₀V₂ after the anion exchange process. Also, as depicted in Fig. S4, the placement of Pd nano-particles in the LDH structure decreases the oxidation peak potential and increases the oxidation peak current of the nano-particles. These results show that collaboration of Pd nano-particles and LDH layers increases the oxidation strength of the nano-particles.

Figure S5 shows the linear sweep voltammetry (LSV) curves of FeCo LDH, FeCo-Pd and FeCo/Mo₁₀V₂-Pd. The onset potentials were evaluated to be 0.392, 0.298 and 0.088 V for FeCo LDH, FeCo-Pd and FeCo/Mo₁₀V₂-Pd, respectively. The comparison of these LSV curves clearly reveals that the FeCo/Mo₁₀V₂-Pd shows a lower onset potential and higher negative limiting current density of -0.35 mA cm⁻². On the basis of the obtained results from the electrocatalytic experiments, we speculate that Mo₁₀V₂, by facilitating the electron transfer by Pd species, intensively helps to enhance the electrocatalytic activity of FeCo/Mo₁₀V₂-Pd in the Heck reaction.

In order to probe the catalytic activity of FeCo/Mo₁₀V₂-Pd and find the best reaction conditions, the reaction of bromobenzene (4 mmol) and styrene (4 mmol) at 120 °C under ligand- and base-free conditions was chosen as a model reaction (Scheme 2).

To establish the best reaction conditions, the amount of FeCo/Mo₁₀V₂-Pd was tested, and it seems that 0.02 g of FeCo/Mo₁₀V₂-Pd was sufficient to drive the reaction in 90% yield. We found that using a smaller amount of FeCo/Mo₁₀V₂-Pd led to a lower yield even with extended reaction time, and increasing in the catalyst quantity showed no significant effect on the productivity of the reaction. Therefore, 0.02 g of the catalyst was chosen as the best amount of FeCo/Mo₁₀V₂-Pd for further reactions (Table 1, entries 1–3). Next, the effects of various solvents, such as H₂O, dimethyl acetamid (DMAc), DMF and mixture of DMF and H₂O, have been studied (entries 1, 4–6). DMF at 120 °C is the best chosen in terms of yield and reaction time (entry 1). The amount of Pd loading on the surface of FeCo/Mo₁₀V₂-Pd as a main catalyst was 6.4 wt%, which was determined using ICP-AES measurements. According to the obtained results from the ICP-AES measurements, the content of Mo was 22.51 wt%, which indicated that the amount of Mo₁₀V₂ in FeCo/Mo₁₀V₂-Pd structure was 40.76 wt%.

To demonstrate the efficiency and generality of FeCo/Mo₁₀V₂-Pd and this process, reaction of a series of aryl halides with styrene was performed under the optimized experimental conditions (Table 2). Each aryl halide containing electron-withdrawing or electron-releasing groups reacts efficiently with styrene for the generation of the corresponding products. Substituent effects on the aromatic ring of the aryl halides had a significant influence on the yield of the reaction. The aryl halides containing electron-withdrawing groups gave corresponding products in higher yields (entries 2 and 5), but aryl halides bearing electron-releasing groups gave the desired products in lower yields (entries 3, 4 and 6). To our surprise, condensation of chlorobenzene with styrene afforded the respective product in a moderate yield (entry 9). It should be pointed out that, when iodobenzene was



Scheme 2 The reaction of styrene and bromobenzene as a model reaction

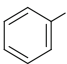
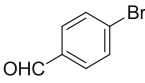
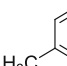
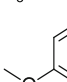
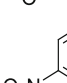
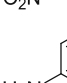
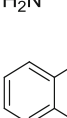
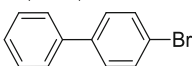
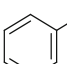
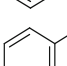
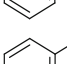
Table 1 Optimization of Mizoroki–Heck coupling reaction conditions

Entry	Amount of the catalyst (mol% of Pd)	Solvent	Time (h)	Yield (%) ^a
1	0.02 g (12×10^{-4})	DMF	8	89
2	0.01 g (6×10^{-4})	DMF	12	75
3	0.03 g (18×10^{-4})	DMF	8	94
4	0.02 g (12×10^{-4})	H ₂ O	24	41
5	0.02 g (12×10^{-4})	DMAc	12	73
6	0.02 g (12×10^{-4})	DMF/H ₂ O (5:1)	12	80

Reaction conditions: styrene (4 mmol), bromobenzene (4 mmol), TBAB (4 mmol) under N₂ atmosphere at 120 °C

^a Isolated yield

Table 2 Mizoroki–Heck reaction of various aryl halides with styrene

Entry	Aryl halide	Time (h)	Yield (%) ^a
1		8	89
2		8	93
3		12	71
4		12	69
5		8	96
6		12	62
7		12	79
8		12	73
9		24	61
10		6	94
11 ^b		8	92

Reaction conditions: Styrene (4 mmol), aryl halide (4 mmol), TBAB (4 mmol) and FeCo/Mo₁₀V₂-Pd (0.02 g) at 120 °C

^a Isolated yield

^b Butylacrylate was used as olefin species

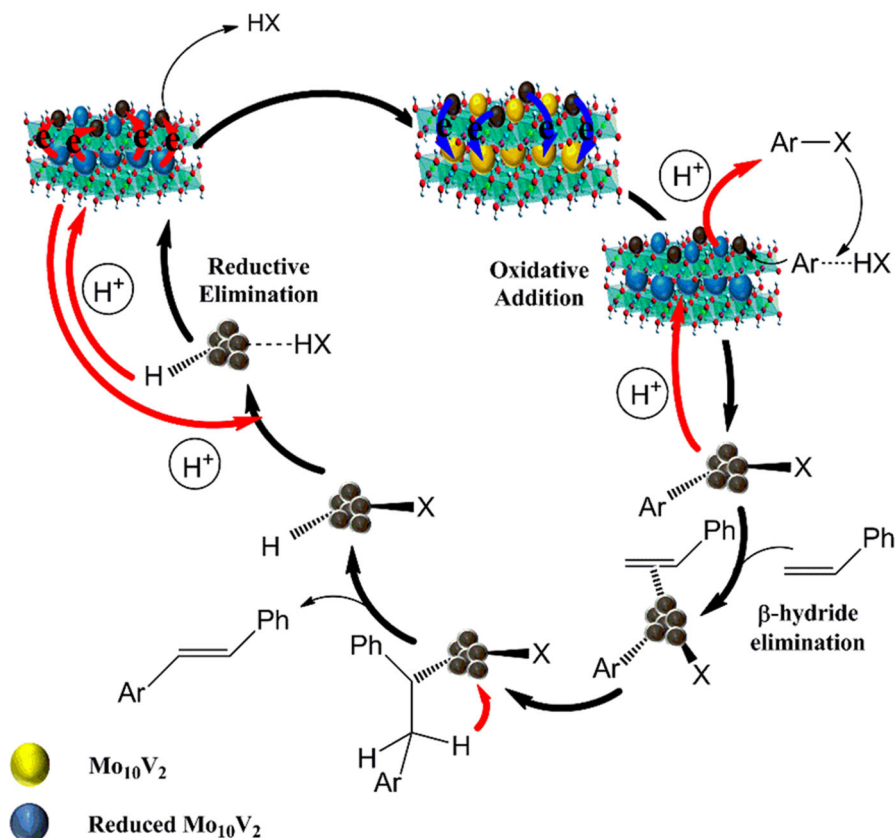
selected as aryl halide, the reaction time was reduced and maximum yield of the desired product was reached (entry 10). The observed higher yield and lower reaction time for the reaction of iodobenzene is due to the strength of the C–I bond which causes the rate of oxidative addition C–I to Pd(0) species to be fast. Also, butylacrylate reacted with bromobenzene efficiently to provide the desired products in maximum yield (entry 11).

The reaction data, along with some literature data for comparison, are given in Table 3. These catalysts showed good reactivity. However, the use of base, ligand and non-recyclable catalysts in these reported systems is not beneficial to industrial and synthetic applications.

For practical application in the Mizoroki–Heck reaction, the lifetime of the heterogeneous catalysts and their reusability are very important factors. After the completion of the reaction, the catalyst was recovered by an external magnet, washed with diethyl ether and water, and reused in a model reaction (Fig. S6). The catalyst revealed a remarkable activity and was reused up to at least four consecutive cycles without any significant decrease in catalytic activity. After the fourth reaction run, the yield of the product decreased from 89 to 77%. According to the obtained results from the XRD and FT-IR techniques, after the completion of the reaction and recovering process, the structure of the FeCo/Mo₁₀V₂-Pd was observed to be unchanged (Figs. 2, S1b, S2c). It is notable that, according to the obtained results from the ICP-AES measurements, after the fourth reaction run, the Pd content in the FeCo/Mo₁₀V₂-Pd structure was evaluated with no significant difference with fresh catalyst.

Table 3 Comparison of the reaction data with other reported methods

Entry	Catalyst	Solvent	Temperature (°C)	Time (h)	Yield (%)	References
1	Pd-Fe ₃ O ₄	DMF	110	24	76	[52]
2	TiO ₂ @Pd	DMF	140	24	91	[53]
3	Benzimidazolium salt/ Pd(OAc) ₂	H ₂ O	100	15	71	[54]
4	Pd(II)/[BMIM][TPPMS]	[BMIM][OAc]	140	3	40	[55]
5	Pd(dba) ₂ /P(OPh) ₃	DMF	100	20	43	[56]
6	Pd(0) MCM-41	DMF	100	24	90	[57]
7	Pd/(SiO ₂ /Fe ₃ O ₄)	CH ₃ CN/H ₂ O	80–90	12	71	[58]
8	NHC-Pd/SBA-16-IL	NMP	140	40	94	[59]
9	Pd/SiO ₂	DMA	135	20	90	[60]
10	FeCo/Mo ₁₀ V ₂ -Pd	DMF	120	8	89	This work



Scheme 3 Proposed mechanism for Heck coupling reaction in the presence of FeCo/ Mo_{10}V_2 -Pd

A possible mechanism for the Mizoroki–Heck reaction in the presence of FeCo/ Mo_{10}V_2 -Pd is presented in Scheme 3. In the first step, the C–X bond of an aryl halide is oxidatively added to the Pd atom. The electron transfer ability of Mo_{10}V_2 facilitates the oxidation of Pd(0) to Pd(II). Pd then forms a π complex with the alkene and, next, the alkene inserts itself into the Pd–carbon bond (Pd–Ar). In the next step, β -hydride elimination causes the formation of a new Pd–alkene π complex. Finally, this complex is destroyed and the desired product is released. The Pd(0) compound is regenerated by reductive elimination of the Pd(II) compound using Mo_{10}V_2 , which could facilitate the reduction of Pd(II) to Pd(0) and eliminate HX by electron transfer and proton donation, respectively.

Conclusion

Here, we have reported the first example of Pd deposited on a FeCo LDH structure with Mo_{10}V_2 anions as the interlayer for using as a catalyst for the Mizoroki–Heck reaction. Characterization of FeCo/ Mo_{10}V_2 -Pd was performed by XRD, FT-IR,

VSM, ICP-AES, SEM and TEM techniques. The CV and LSV investigations show that the presence of Mo_{10}V_2 is essential because it can probably activate precursors of the reaction and may transfer the electrons with Pd species which facilitates the oxidation of Pd(0) in the oxidative addition and regeneration of Pd(II) species in the reductive elimination steps. $\text{FeCo/Mo}_{10}\text{V}_2\text{-Pd}$ can easily be recovered using an external magnet. The study of the catalytic properties of the sample exhibits high activity for the Mizoroki–Heck reaction.

Acknowledgements The authors thank the Razi University Research Council and Iran National Science Foundation (INSF) for support of this work.

References

1. G.T. Crisp, *Chem. Soc. Rev.* **27**, 6 (1998)
2. N.J. Whitcombe, K.K.M. Hii, S.E. Gibson, *Tetrahedron* **57**, 35 (2001)
3. I. Beletskaya, A. Cheprakov, *Chem. Rev.* **100**(8), 3009–3066 (2000)
4. S.S. Pröckl, W. Kleist, M.A. Gruber, K. Köhler, *Angew. Chem. Int. Ed.* **43**, 1881 (2004)
5. C.S. Consorti, F.R. Flores, J. Dupont, *J. Am. Chem. Soc.* **127**, 12054 (2005)
6. A. Zapf, M. Beller, *Chem. Commun.*, 431 (2005)
7. K. Gholivand, M. Kahnouji, S. Mark Roe, A. Gholami, F.T. Fadaei, *Appl. Organomet. Chem.* (2017). doi:[10.1002/aoc.3793](https://doi.org/10.1002/aoc.3793)
8. V. Sable, K. Maingan, A.R. Kapdi, P.S. Shejwalkar, K. Hara, *ACS Omega* **2**, 1 (2017)
9. J. Mo, L. Xu, J. Ruan, S. Liu, J. Xiao, *Chem. Commun.*, 3591 (2006)
10. S. Kim, H.-J. Cho, D.-S. Shin, S.-M. Lee, *Tetrahedron Lett.* **58**, 2421 (2017)
11. M.R. Nabid, Y. Bide, S.J.T. Tezaei, *Appl. Catal. A Gen.* **406**, 15 (2011)
12. K.N. Ali, P. Farhad, *Green Chem.* **13**, 2247 (2011)
13. J.D. Senra, A.C. Silva, R.V. Santos, L.F.B. Malta, A.B. Simas, *J. Chem.* (2017). doi:[10.1155/2017/8418939](https://doi.org/10.1155/2017/8418939)
14. B.M. Choudary, S. Madhi, N.S. Chowdari, M.L. Kantam, B. Sreedhar, *J. Am. Chem. Soc.* **124**, 47 (2002)
15. B. Choudary, M.L. Kantam, N.M. Reddy, N. Gupta, *Catal. Lett.* **82**, 1 (2002)
16. F. Cavani, F. Trifiro, A. Vaccari, *Catal. Today* **11**, 173 (1991)
17. N.K. Lazaridis, T.A. Pandi, K.A. Matis, *Ind. Eng. Chem. Res.* **43**(9), 2247 (2004)
18. J.H. Choy, S.Y. Kwak, Y.J. Jeong, J.S. Park, *Angew. Chem. Int. Ed.* **39**, 4041 (2000)
19. L. Li, R.Z. Ma, Y. Ebina, N. Lyi, T. Sasaki, *Chem. Mater.* **17**(17), 4386 (2005)
20. M. Hajibeygi, M. Omid-Ghallemohamadi, *J. Polym. Res.* **24**, 4 (2017)
21. H.R. Mardani, *Res. Chem. Intermed.* (2017). doi:[10.1007/s11164-017-2963-y](https://doi.org/10.1007/s11164-017-2963-y)
22. B. Bi, L. Xu, B. Xu, X. Liu, *Appl. Clay Sci.* **54**, 242 (2011)
23. P. Liu, C. Wang, C. Li, *J. Catal.* **262**, 159 (2009)
24. C.-W. Chiu, T.-K. Huang, Y.-C. Wang, B.G. Alamani, J.-J. Lin, *Prog. Polym. Sci.* **39**(3), 443 (2014)
25. L. Mohapatra, D. Patra, K. Parida, S.J. Zaidi, *Eur. J. Inorg. Chem.* **2017**, 723 (2017)
26. S. Ryo, M. Morita, *Sens. Actuators B Chem.* **238**, 702 (2017)
27. W. Liu, N. Liang, P. Peng, R. Qu, D. Chen, H. Zhang, *J. Solid State Chem.* **246**, 324 (2017)
28. M. Zubair, M. Daud, G. McKay, F. Shehzad, M.A. Al-Harhi, *Appl. Clay Sci.* **143**, 279 (2017)
29. Y. Guo, D. Li, C. Hu, Y. Wang, E. Wang, *Int. J. Inorg. Mater.* **3**, 347 (2001)
30. Y. Watanabe, K. Yamamoto, T. Tatsumi, *J. Mol. Catal. A Chem.* **145**, 281 (1999)
31. P. Liu, H. Wang, Z. Feng, P. Ying, C. Li, *J. Catal.* **256**, 2 (2008)
32. Q. Wang, D. O'Hare, *Chem. Rev.* **112**, 7 (2012)
33. D. Tonelli, E. Scavetta, M. Giorgetti, *Anal. Chem.* **405**, 2 (2013)
34. A. Leuteritz, B. Kutlu, J. Meinl, D. Wang, A. Das, U. Wagenknecht, G. Heinrich, *Mol. Cryst. Liq. Cryst.* **556**, 1 (2012)
35. C. Del Hoyo, *Appl. Clay Sci.* **36**, 1 (2007)

36. X. Liang, Y. Zang, Y. Xu, X. Tan, W. Hou, L. Wang, Y. Sun, *Colloids. Surf. A Physicochem. Eng. Asp.* **433**, 122 (2013)
37. L. Kaitao, W. Guirong, L. Dianqing, L. Yanjun, D. Xue, *Chin. J. Chem. Eng.* **21**, 4 (2013)
38. E. Akbarzadeh, M.R. Gholami, *Res. Chem. Intermed.* (2017). doi:[10.1007/s11164-017-2965-9](https://doi.org/10.1007/s11164-017-2965-9)
39. M. Kotal, A.K. Bhowmick, *Prog. Polymer Sci.* **51**, 127 (2015)
40. M.T. Pope, *Heteropoly and Isopoly Oxometalates* (Springer, Berlin, 1983)
41. K. Fukaya, T. Yamase, *Angew. Chem.* **115**, 678 (2003)
42. M.T. Pope, *Heteropoly and Isopolyoxometalates* (Springer-Verlag, New York, 1983)
43. N. Mizuno, M. Misono, *Chem. Rev.* **98**, 199 (1998)
44. D. Drewes, E.M. Limanski, B. Krebs, *Dalton Trans.* **14**, 2087 (2004)
45. E. Rafiee, M. Kahrizi, *J. Mol. Liq.* **218**, 625 (2016)
46. E. Rafiee, M. Kahrizi, *Res. Chem. Intermed.* **42**, 2833 (2016)
47. E. Rafiee, M. Kahrizi, M. Joshaghani, P.G.-S. Abadi, *Res. Chem. Intermed.* **42**, 5573 (2016)
48. A. Corma, S. Iborra, I. Llabres, F.X. Xamena, R. Monton, J.J. Calvino, C. Prestipino, *J. Phys. Chem. C* **114**, 8828 (2010)
49. E. Rafiee, A. Ataei, S. Nadri, M. Joshaghani, S. Eavani, *Inorg. Chim. Acta* **409**, 302 (2014)
50. R. Ma, Z. Liu, K. Takada, *J. Am. Chem. Soc.* **129**, 5257 (2007)
51. V. Rives, M.A. Ulibarri, *Coord. Chem. Rev.* **181**, 61 (1999)
52. J. Chung, J. Kim, Y. Jang, S. Byun, T. Hyeon, B.M. Kim, *Tetrahedron Lett.* **54**, 38 (2013)
53. M. Nasrollahzadeh, A. Azarian, A. Ehsani, M. Khalaj, *J. Mol. Catal. A: Chem.* **394**, 205 (2014)
54. A. Slamani, S. Demir, İ. Özdemir, *Catal. Commun.* **29**, 141 (2012)
55. Y. Liu, M. Li, Y. Lu, G.-H. Gao, Q. Yang, M.-Y. He, *Catal. Commun.* **7**, 12 (2006)
56. J.C. Cárdenas, L. Fadini, C.A. Sierra, *Tetrahedron Lett.* **51**, 52 (2010)
57. S. Jana, B. Dutta, R. Bera, S. Koner, *Inorg. Chem.* **47**, 12 (2008)
58. Z. Wang, P. Xiao, B. Shen, N. He, *Colloids Surf. A Physicochem. Eng. Asp.* **276**, 1 (2006)
59. H. Yang, X. Han, G. Li, Y. Wang, *Green Chem.* **11**, 8 (2009)
60. L. Huang, Z. Wang, T. Ang, J. Tan, P. Wong, *Catal. Lett.* **112**, 3 (2006)